

## RADIAL ABUNDANCE GRADIENTS FROM PLANETARY NEBULAE AT DIFFERENT DISTANCES FROM THE GALACTIC PLANE

W. J. Maciel,<sup>1</sup> R. D. D. Costa,<sup>1</sup> and O. Cavichia<sup>2</sup>

Received December 18 2014; accepted March 9 2015

### RESUMEN

Investigamos las variaciones de los gradientes radiales de abundancia de O/H de nebulosas planetarias (PN) situadas a diferentes distancias del plano galáctico. En particular, determinamos los gradientes de abundancia a diferentes alturas del plano con el fin de investigar una posible inversión del gradiente en los objetos más distantes. Consideramos una amplia muestra de PN con distancias conocidas para así poder derivar la altura relativa al plano galáctico, así como las abundancias exactas, que son necesarias para determinar los gradientes.

### ABSTRACT

We studied the variations of the radial O/H abundance gradients from planetary nebulae (PN) located at different distances from the galactic plane. In particular, we determined the abundance gradients at different heights from the plane in order to investigate a possible gradient inversion for the objects at larger distances from the plane. We considered a large sample of PN with known distances, so that the height relative to the galactic plane can be obtained and with accurate abundances, so that the abundance gradients can be determined.

*Key Words:* Galaxy: abundances — Galaxy: disk — ISM: abundances — planetary nebulae: general

### 1. INTRODUCTION

There is evidence that the galactic radial abundance gradient of elements such as Fe, O, etc., changes according to the ages of the objects considered. Two main changes have been suggested in the literature: first, the average abundances decrease with the age of the objects considered, while the gradient itself may or may not be affected. Second, there is evidence indicating that there is an inversion of the gradients in older objects at low galactocentric distances,  $R < 8$  kpc, meaning that outwardly decreasing abundances also decrease inwards as older objects are considered (Sancho-Miranda et al. 2014, Cheng et al. 2012a, 2012b, Carrell et al. 2012).

The results by Cheng et al. (2012a, 2012b) suggest that the radial gradients flatten out at large distances from the galactic plane, which was confirmed by Carrell et al. (2012) in a sample of dwarf stars from the SEGUE survey at  $7 < R(\text{kpc}) < 10.5$ , with proper motions and spectroscopic abundances. That

survey included objects up to  $|z| \simeq 3$  kpc, for which a slightly positive gradient of the [Fe/H] ratio was obtained. Other studies of thick disk stars also found flat or slightly positive gradients (Allende-Prieto et al. 2006, Nordström et al. 2004).

Some recent chemical evolution models predict a strong flattening of the [Fe/H] radial gradient at greater distances from the galactic plane ( $|z| > 0.5$  kpc), as shown for example by Minchev et al. (2014), see also Chiappini et al. (2015) and references therein. These models take into account radial migration and suggest an inversion of the gradient from negative to weakly positive for  $R < 10$  kpc and  $0.5 < |z| < 1.0$  kpc. Theoretical models by Curir et al. (2012) and Spitoni & Matteucci (2011) also predict an inversion of the gradient at galactocentric distances of about 10 kpc for the early Galaxy (about 2 Gyr), a consequence of the inside-out formation of the thick disk.

Differences in the radial abundance gradients are also supported by Fe/H and Si/H gradients derived from red clump stars from the RAVE survey, the steeper gradients occurring at short distances to the

<sup>1</sup>Instituto de Astronomia, Geofísica e Ciências Atmosféricas, Universidade de São Paulo, Brazil.

<sup>2</sup>Instituto de Física e Química, Universidade Federal de Itajubá, Brazil.

galactic plane, and becoming flatter for higher  $z$  values. A slightly positive gradient was derived from APOGEE data for stars at  $1.5 < z(\text{kpc}) < 3.0$  (Chiappini et al. 2015, Boeche et al. 2014).

Planetary nebulae may contribute to this problem. The nebulae located in the disk of the Galaxy are spread along at least 1 kpc above (or below) the galactic plane, that is, these objects have typically  $0 < |z|(\text{pc}) < 1,000$ . In view of the number of PN with known abundances, about 300 objects, it is possible that some differences between the derived gradients may be found when objects at different heights from the plane are considered. In principle, PN located higher above the galactic plane are produced by older stars, as in the case of the halo PN, which are very probably older than the disk nebulae.

In this work, we investigated possible variations in the radial abundance gradients of objects at different distances from the galactic plane. We examined a large sample of galactic PN with known distances and accurate abundances, to determine both their  $z$  height relative to the galactic plane and the galactocentric distance  $R$  independently of the radial abundance gradients. We considered the oxygen abundance ratio O/H, which has been derived for a large number of objects and has the smallest uncertainties among all known abundances.

## 2. THE DATA

The main problem in studying gradients from planetary nebulae is to obtain their distances. In this study, we considered objects from the Magellanic Cloud calibration by Stanghellini et al. (2008) and, in particular from Stanghellini & Haywood (2010, hereafter SH), who also estimated chemical abundances. This is the most recent sizable distance scale in the literature, so that the probability of obtaining a reasonable estimate of the gradients was higher. Table 1 of Stanghellini and Haywood (2010) includes 728 objects, which were our starting sample. The objects are referenced by their PNG number, to which we added the common names from the catalogue by Acker et al. (1992). Table 2 of Stanghellini and Haywood (2010) gives nebular abundances of He, N, O, and Ne for a smaller sample, containing 224 objects. Since the galactic coordinates  $(l, b)$  are known, it was possible to obtain the  $z$  coordinate and the galactocentric distance  $R$  by taking into account the distances, choosing  $R_0 = 8 \text{ kpc}$  as the distance of the Sun to the galactic center. As an alternative to the abundances given by SH, we also considered the abundances given by the IAG group as discussed, for example, by Maciel and Costa (2013). This included

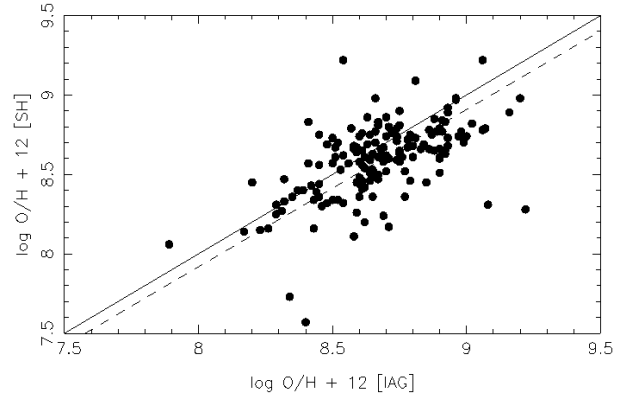


Fig. 1. Comparison of the oxygen abundances found by Stanghellini & Haywood (2010) ( $y$  axis) and the abundances estimated from the IAG sample ( $x$  axis).

234 disk nebulae. Considering the objects of both samples as part of the 728 PN sample given by SH, oxygen abundances are known for 201 objects from the SH sample; 222 objects from the IAG sample; 160 objects from both the SH and IAG samples, and 263 of all objects with abundances in at least one of the two samples. This was the initial sample of galactic disk planetary nebulae that we considered in this study.

The reason why we could safely include the oxygen chemical abundances from both samples (SH and IAG) can be seen in Figure 1, where we plotted SH oxygen abundances ( $y$  axis) as a function of the IAG abundances ( $x$  axis). A linear fit of the form  $y = ax$  gives the following results:  $a = 0.9898$ , with a standard deviation  $\sigma = 0.0019$ , and correlation coefficient  $r = 0.9997$ , with an uncertainty  $\sigma_r = 0.2096$ . The least squares fit line (dashed line) is very close to the one-to-one line (full line), only slightly displaced downwards by about 0.05 dex. It can be seen that only a few nebulae have deviations higher than the average.

## 3. THE METHOD

In order to study the possible variations of the abundance gradient in older objects, which are in principle located higher above the galactic plane, we divided the sample of 263 objects into several groups according to their  $z$  values and compared the results of each group with the whole sample. After defining the groups, the procedure consisted in plotting  $\epsilon(\text{O}) = \log \text{O}/\text{H} + 12$  as a function of the galactocentric distance  $R$ , estimating the average linear gradient with the equation

$$\epsilon(\text{O}) = \log \text{O}/\text{H} + 12 = A + B R \quad (1)$$

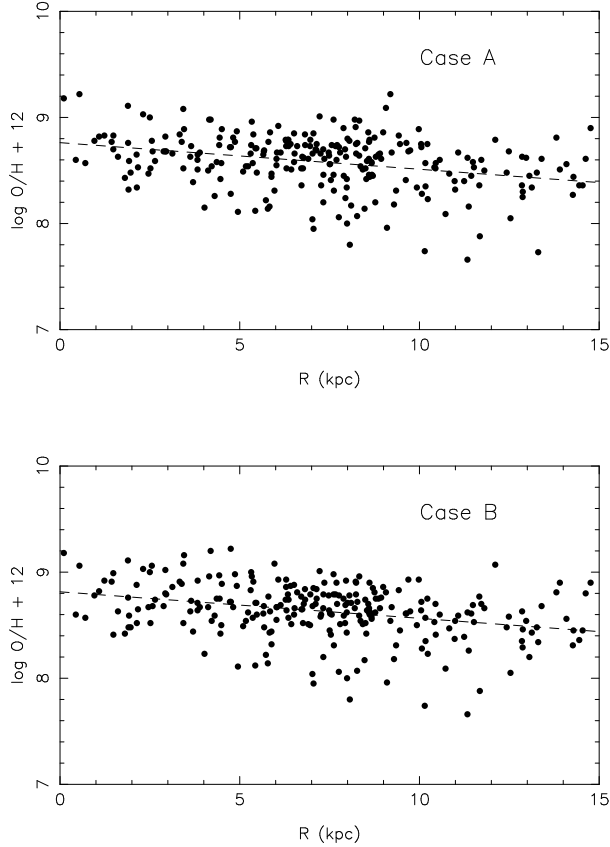


Fig. 2. Variation of oxygen abundance according to galactocentric distance of the whole sample; Cases A and B.

and then estimating the coefficients  $A$  and  $B$ , their uncertainties and the correlation coefficient  $r$ . We were also interested in investigating any possible variation of the slope  $B$  along the galactocentric radius, thus we also obtained polynomial fits using a second degree function defined as

$$\epsilon(\text{O}) = C + D R + E R^2 \quad (2)$$

and then estimated the coefficients  $C$ ,  $D$ ,  $E$ , as well as the  $\chi$  squared value. We considered two cases: Case A, in which we used the abundances given by SH when both samples had abundances for the same object, and Case B, in which we used the abundances from the IAG sample. As it turned out, Case A and B produced essentially the same results; thus most figures presented here are for Case A.

## 4. RESULTS AND DISCUSSION

### 4.1. The Total Disk Sample

The first results were obtained for the whole sample of 263 objects, both for Case A and B. The linear

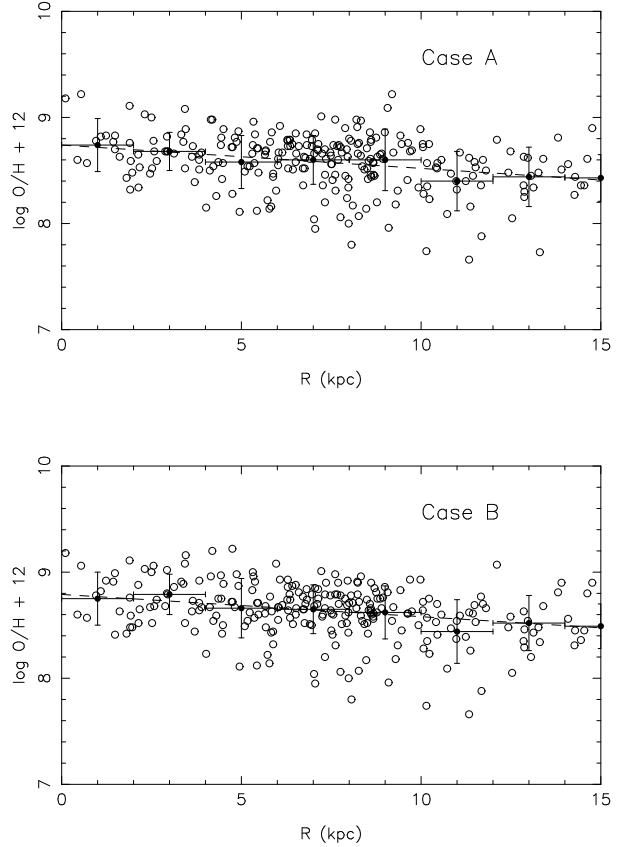


Fig. 3. The same as Figure 2, adopting average abundances in 2 kpc bins.

fits to equation (1) are shown in the first two rows of Table 1. The corresponding figures are shown in Figure 2; they include objects up to 15 kpc from the center, so that a few objects at higher galactocentric distances were not included. It can be seen that in both cases, an average gradient of  $d(\text{O}/\text{H})/dR \simeq -0.02$  to  $-0.03$  dex/kpc is obtained. The average uncertainty in the abundances was about  $-0.2$  dex. The dispersion was greater at larger galactocentric distances, as expected, while the correlation coefficient was relatively low, which is a consequence of the relatively flat gradient and of the uncertainties in the abundances.

We could probably obtain a more meaningful result by dividing the sample according to the galactocentric distances of each object, for example using 2 kpc bins. We considered 9 bins, and the results are shown in Figure 3, where the data points are shown as empty circles and the average abundances in each bin as filled circles. The vertical error bars show the mean deviation and the horizontal bars show the

TABLE 1  
COEFFICIENTS OF THE LINEAR FITS TO EQUATION (1)

Case	$A$	$\sigma_A$	$B$	$\sigma_B$	$r$	$\sigma_r$
all data						
A	8.7625	0.0349	-0.0251	0.0041	-0.3565	0.2529
B	8.8146	0.0342	-0.0250	0.0040	-0.3626	0.2474
binned data						
A	8.7390	0.0316	-0.0223	0.0029	-0.9443	0.0487
B	8.7885	0.0344	-0.0213	0.0032	-0.9289	0.0532
disk + bulge nebulae						
A	8.6596	0.0265	-0.0156	0.0035	-0.2292	0.2731
B	8.6780	0.0266	-0.0124	0.0035	-0.1828	0.2743

selected galactocentric thresholds. The dashed line shows the linear fits as indicated in Rows 3 and 4 of Table 1.

A comparison of the dashed lines in Figures 2 and 3 shows that they are very similar, that is, the linear fits of the whole sample and of the binned data are essentially the same. This can also be seen from Table 1, which shows that the intercept and slope of both lines are very similar. However, the correlation coefficients of the binned data are much higher than those of the whole sample.

A more detailed analysis can be made by obtaining a polynomial fit to the data, so that any variation of the slope due to a change of position can be estimated. We considered a second order polynomial fit to the data, as defined in equation (2). The obtained coefficients are  $C = 8.7581$ ,  $D = -0.0238$ , and  $E = -0.0001$  for Case A, with  $\chi = 0.0643$ , and  $C = 8.8364$ ,  $D = -0.0312$ , and  $E = 0.0004$  with  $\chi = 0.0614$  for Case B. In Case A the linear and quadratic fits are almost the same, while in Case B there is a slight difference between them for  $R > 10$  kpc. In addition, in Case A the gradients are essentially constant for the whole range of galactocentric distances, while some flattening is observed at large  $R$  in Case B. The gradient varies from  $d(\text{O}/\text{H})/dR \simeq -0.024$  to  $-0.027$  dex/kpc in Case A, with similar results in Case B.

Considering the total sample of disk objects, it can be seen that the average gradients found here are similar or somewhat flatter than previous deter-

minations (e.g. Maciel & Costa 2013). Since PNe are relatively old objects, compared for example with HII regions, they may have been displaced from their original birthplaces. As a consequence, the measured gradients are probably flatter than before the displacement occurred. In other words, gradients derived from planetary nebulae are probably a lower limit of the original gradient. In fact, simulations with a large number of objects show that there is no way the gradients could increase due to the displacement of the progenitor stars. In addition, most PN samples considered so far in the literature include objects of very different ages, as we showed in our previous work on the age determination of the PN progenitor stars (Maciel et al. 2010 2011; Maciel & Costa 2013); this also contributes to the flattening of the gradients.

Some recent chemodynamical models (e.g. Chiappini et al. 2015, and references therein) suggest that the solar neighbourhood has been contaminated with stars born at smaller galactocentric distances; these stars are more metal-rich, since they come from a more metal-rich environment. As a result, a determination of the gradient based on relatively old stars, such as PN progenitor stars, leads to a flatter gradient. In fact, radial migration has been proposed as a common phenomenon in the history of the Milky Way, and models exploring this characteristic have been able to explain several chemical evolution constraints, such as the metallicity distribution and radial gradients (cf. Schönrich & Binney 2009).

TABLE 2  
DEFINITION OF THE HEIGHT GROUPS

Number of groups	Group	height (pc)
2	1	$ z  \leq 1,000$
	2	$ z  > 1,000$
2	1	$ z  \leq 800$
	2	$ z  > 800$
2	1	$ z  \leq 600$
	2	$ z  > 600$
3	1	$ z  \leq 500$
	2	$1000 \geq  z  > 500$
	3	$ z  > 1,000$
4	1	$ z  \leq 500$
	2	$1,000 \geq  z  > 500$
	3	$1,500 \geq  z  > 1,000$
	4	$ z  > 1,500$
6	1	$ z  \leq 400$
	2	$800 \geq  z  > 400$
	3	$1,200 \geq  z  > 800$
	4	$1,600 \geq  z  > 1,200$
	5	$2,000 \geq  z  > 1,600$
	6	$ z  > 2,000$
11	1	$ z  \leq 200$
	2	$400 \geq  z  > 200$
	3	$600 \geq  z  > 400$
	4	$800 \geq  z  > 600$
	5	$1,000 \geq  z  > 800$
	6	$1,200 \geq  z  > 1,000$
	7	$1,400 \geq  z  > 1,200$
	8	$1,600 \geq  z  > 1,400$
	9	$1,800 \geq  z  > 1,600$
	10	$2,000 \geq  z  > 1,800$
	11	$z > 2000$

4.2. The Disk Sample Divided into Height Groups

The groups were defined by taking steps of 1,000 pc, 600 pc, 500 pc, 400 pc, and 200 pc: 2 groups ( $\Delta = 1,000$  pc, 800 pc, and 600 pc); 3 groups ( $\Delta = 500$  pc); 4 groups ( $\Delta = 500$  pc); 6 groups ( $\Delta = 400$  pc), and 11 groups ( $\Delta = 200$  pc). A detailed description of the groups is given in Table 2.

In view of the relatively small size of the sample considered, it was unlikely that a division into many groups would produce meaningful results, since the

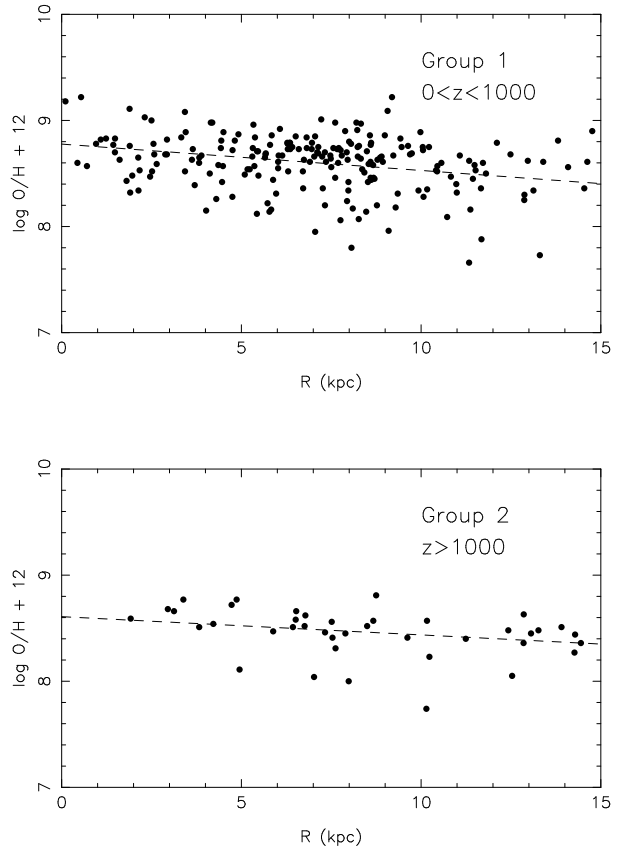


Fig. 4. The same as Figure 2, using 2 height groups with  $\Delta = 1,000$  pc, Case A.

number of objects at each height would be small; thus we focused on the division into 2 groups.

We considered first what was probably the most meaningful result, namely, the division into 2 groups, with steps of 1,000 pc; that is, Group 1 has  $|z| \leq 1,000$  pc and Group 2 has  $|z| > 1,000$  pc. This limit provides an approximate separation of the thin disk and the thick disk. The main results are shown in the first two rows of Table 3 (Case A), and in the plots shown in Figure 4. We can derive the following conclusions:

1. The intercept of Group 1 is higher than that of Group 2, meaning that the abundances of Group 1 are somewhat higher than those of Group 2, as expected if the former is younger than the latter. It can also be seen that Group 2 tends to have lower abundances than Group 1.
2. The gradient of Group 1 is slightly steeper than that of Group 2, but if the uncertainties are taken into account both gradients are essentially the same, that is, it is probably not possible to conclude

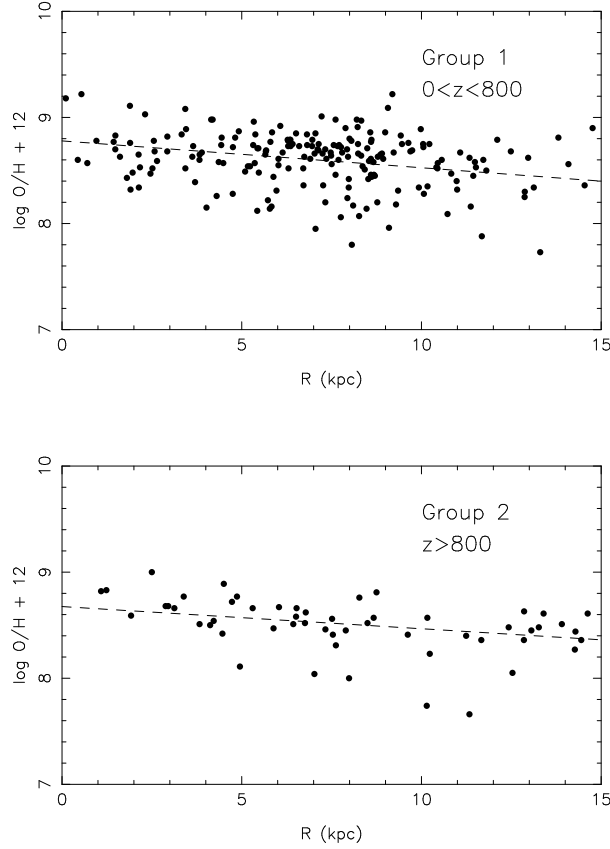


Fig. 5. The same as Figure 2, using 2 height groups with  $\Delta = 800$  pc, Case A.

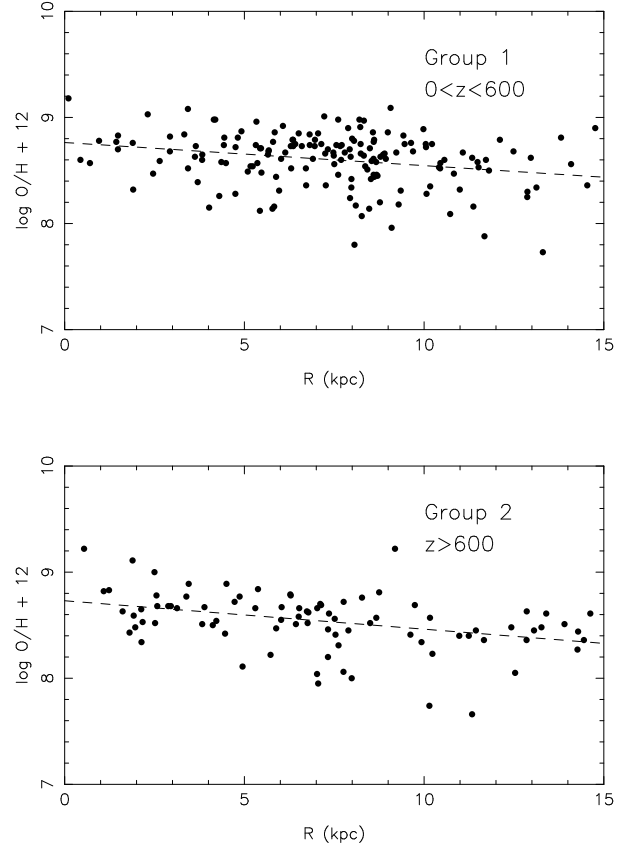


Fig. 6. The same as Figure 2, considering 2 height groups with  $\Delta = 600$  pc, Case A.

that the objects at lower heights have gradients different from those at higher  $z$  values. Again, the correlation coefficients are small.

3. There is no evidence of any inversion of the gradient at small galactocentric distances. It should be mentioned that the samples considered so far do not include objects belonging to the galactic bulge (see § 4).

Considering now the other divisions into two groups, shown in the remaining rows of Table 3 and in Figures 5 and 6, it can be seen that Conclusions 1 and 3 above are still valid, but Conclusion 2 differs somewhat for the groups having  $\Delta = 600$  pc, in that the gradient of Group 2 is slightly steeper than that of Group 1. However, the difference is again small, so that Conclusion 2 above is also valid for both groups.

The division into 3 groups was the same as in the previous case for  $\Delta = 1,000$  pc, except that Group 1 is further subdivided into 2 groups. The results are similar, but clearly the new Group 2 has relatively few objects compared with the new Group 1. The division into 4 groups was also the same, except that

both groups are further subdivided into 2 groups. The main difference from the previous results is that the new Group 3 has very few objects, thus showing no gradient at all. In the division into 6 groups we noticed that Groups 4 and 5 had now very few objects, so that their gradient was meaningless. Otherwise, the results were similar to the previous cases. In the division into 11 groups, Groups 6 to 10 have very few objects, so that their gradients were also meaningless. Otherwise, the results were similar to the previous cases.

The results of § 4.1 are reinforced by the oxygen and neon gradients determined by Stanghellini and Haywood (2010), who obtained different estimates for Peimbert Type I, II, and III objects. Their procedure implicitly assumed that the gradients were derived at different epochs, since Type I, II and III objects are expected to reflect the increasing ages of the progenitor stars. It was found that the gradients of Type III nebulae, which are in principle located higher above the galactic disk, were slightly flatter, although the differences in the gradients were small

and similar to those found in the present work. Comparing the results of SH with the present results for objects at different heights from the galactic plane, it can be seen that our gradients at high  $|z|$  are typically of  $-0.017$  dex/kpc, or slightly steeper, very similar to the Type III gradients derived by SH, namely  $-0.011$  dex/kpc. For the objects closer to the disk, we estimated a gradient of  $-0.025$  dex/kpc, while SH derived  $-0.035$  dex/kpc for Type I nebulae; for the intermediate mass population the corresponding gradients were about  $-0.021$  dex/kpc, closer to the SH values of  $-0.023$  dex/kpc for Type II objects. Thus, this is a confirmation that the Peimbert types as originally defined by Peimbert (1978), with a few posterior updates, reflect the main population characteristics of the PN in the Galaxy.

#### 4.3. The Extended Sample: Disk, Bulge, and Interface Region

The previous samples include mostly objects in the galactic disk, but there are many PN known to be in the galactic bulge or in the interface region. The distinction is not always clear, especially because of the uncertainties in the distances. Therefore, it would be interesting to include these objects in our analysis, although some care must be taken to distinguish them from the previous samples of disk planetary nebulae.

Our own IAG sample included 179 objects that in principle belong to the bulge population or to the disk interface (e.g. Cavichia et al. 2010, 2011, 2014, 2015). Ninety-four objects from this sample had distances from Stanghellini et al. (2008). The abundances were taken from the IAG sample, as these objects were not included in the SH sample. Considering these objects, we had a total sample of  $263+94=357$  nebulae.

The main results are shown in Figure 7; the filled circles are data of the disk and the empty circles are data of the bulge/interface region. The latter included objects up to about  $R = 6$  kpc, so that some of these objects are clearly not in the galactic center. It can be seen that the inclusion of bulge/interface data makes the gradients somewhat smaller compared with the average gradients measured in the outer disk, so that the trend observed for  $R > 3 - 4$  kpc is somewhat modified. This effect should not be confused with a possible inversion of the gradient at large  $z$ -heights from the plane, since the bulge/interface objects are located

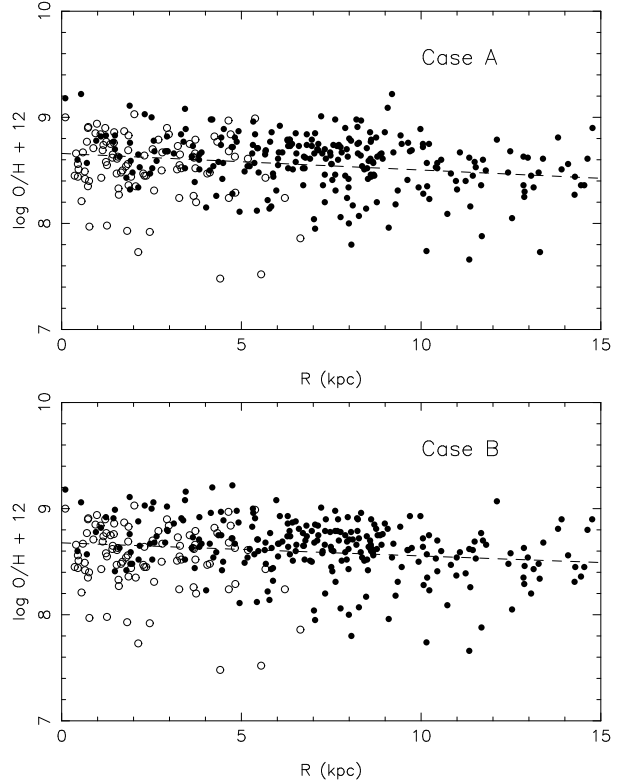


Fig. 7. The same as Figure 2, including objects from the bulge/disk interface region.

very close to the galactic plane. A similar distribution of bulge nebulae on the O/H vs  $R$  plane was observed by Gutenkunst et al. (2008). It should be noted that some objects show lower abundances ( $\log O/H + 12 < 8$ ) than expected according to the trend defined by most nebulae in both samples. It is possible that these objects can be explained by local abundance variations or by the fact that the corresponding central stars are older than most progenitor stars in the sample. In addition, in this region the galactic bar may play an important role in the shaping of the gradient (cf. Cavichia et al. 2014).

The linear fits are also shown in the last two rows of Table 1, again for Cases A and B. The slopes are still of the order of  $-0.02$  dex/kpc, slightly lower than for the previous cases, but they were probably affected by the low abundance objects mentioned above. The gradients became closer to the disk sample when we excluded the outliers. We were able to obtain a polynomial fit to the data as in the previous case. The results are similar, and the gradients varied from a minimum of  $-0.014$  dex/kpc to  $-0.037$  dex/kpc for Case A, with similar results for Case B.

TABLE 3  
COEFFICIENTS OF THE LINEAR FITS ADOPTING TWO HEIGHT GROUPS.

	$A$	$\sigma_A$	$B$	$\sigma_B$	$r$	$\sigma_r$
$\Delta = 1,000$ pc						
Group 1: $n = 218$	8.7773	0.0395	-0.0248	0.0048	-0.3300	0.2600
Group 2: $n = 45$	8.6086	0.0756	-0.0172	0.0073	-0.3400	0.2100
$\Delta = 800$ pc						
Group 1: $n = 202$	8.7790	0.0424	-0.0253	0.0053	-0.3200	0.2600
Group 2: $n = 61$	8.6755	0.0661	-0.0209	0.0065	-0.3900	0.2400
$\Delta = 600$ pc						
Group 1: $n = 168$	8.7639	0.0480	-0.0218	0.0059	-0.2800	0.2500
Group 2: $n = 95$	8.7302	0.0529	-0.0268	0.0057	-0.4400	0.2600

#### 4.4. Final Remarks

Conclusions 1-3, listed in § 4.2, are in good agreement with our previous results on the time variation of the abundance gradient (Maciel & Costa 2013). In particular, Conclusion 1 states the observed differences in the average abundances of PN at high  $z$  (older objects) and low  $z$  (younger objects), while Conclusion 2 states the similarity of the gradients of both groups. The first conclusion is consistent with the existence of a vertical abundance gradient, as found in thin and thick disk stars of the Milky Way based on stellar data (e.g. Carrell et al. 2012, Chen et al. 2011). Maciel & Costa (2013) considered four samples of galactic PN for which the ages of their progenitor stars were estimated using three different methods. They concluded that the younger objects had similar or somewhat higher oxygen abundances compared with the older objects, but the gradients were similar within the uncertainties. The actual magnitudes of the gradients are in the range  $-0.03$  to  $-0.07$  dex/kpc with an average of  $-0.05$  dex/kpc, but they depend on the sample used. The results of the present paper are closer to the lower limit, which is probably a consequence of the adopted distance scale and of the effects of radial migration. Conclusion 2 is also supported by the results of Henry et al. (2010), who divided their planetary nebula sample into two groups using a threshold of  $z = 300$  pc. Again, the slope of the group closer to the galactic plane is slightly steeper, but the distributions of the two subsamples were essentially the same.

Similar conclusions were reached in our recent work on the abundance gradients as measured in

symmetric and asymmetric PN (Maciel & Costa 2014). Since asymmetric PN, especially bipolars, are generally considered to be younger than the symmetric objects, some difference in their gradients should probably be observed in sufficiently large samples. Considering the gradients of elements O, Ne, S, and Ar, we concluded that the average abundances of bipolar nebulae are somewhat higher than for non-bipolars for all elements studied, confirming our Conclusion 1 above; however, no important differences were found between the gradients, which were in the range of  $-0.03$  to  $-0.05$  dex/kpc for oxygen. These results are also supported by recent work by Pilkington et al. (2012) and Gibson et al. (2013), who concluded that there are no appreciable differences in the gradients of objects in the local universe, at near zero redshift, although steeper gradients are expected at much higher redshifts, beyond the age bracket considered in the present paper.

Cheng et al. (2012a, 2012b) considered the Fe/H abundances of a large sample of main sequence turnoff stars from the SEGUE survey in the region of galactocentric distances  $6 < R(\text{kpc}) < 16$  and heights relative to the galactic plane of  $150 < |z|(\text{pc}) < 1500$ . They found that the Fe gradient was about  $-0.06$  dex/kpc close to the disk ( $|z| < 1500$  pc), while for higher distances from the plane, of  $|z| > 1,000$  pc, the gradient flattened out, showing a negligible slope. Their sample was limited to objects with  $R > 6$  kpc, and thus no information was provided about a possible gradient inversion in the inner disk. Since the Fe gradient is probably slightly steeper than the oxygen gradient (see a dis-

cussion of this in Maciel et al. 2013), it can be concluded that their results are generally in agreement with our present results.

We are indebted to an anonymous referee for some interesting comments and suggestions on a previous version of this paper. This work was partially supported by FAPESP and CNPq.

## REFERENCES

- Acker, A., Marcout, J., Ochsenbein, F., Stenholm, B., Tylenda, R., & Schohn, C. 1992, The Strasbourg-ESO catalogue of galactic planetary nebulae
- Allende-Prieto, C., Beers, T. C., Wilhelm, R. et al. 2006, *ApJ*, 636, 804
- Boeche, C., Siebert, A., Piffl, T. et al. 2014, *A&A*, 568, A71
- Carrell, K., Chen, Y., Zhao, G. 2012, *AJ*, 144, 185
- Cavichia, O., Costa, R. D. D., & Maciel, W. J. 2010, *RMxAA*, 46, 159
- \_\_\_\_\_. 2011, *RMxAA*, 47, 49
- Cavichia, O., Mollá, M., Costa, R. D. D., & Maciel, W. J. 2014, *MNRAS*, 437, 3688
- Cavichia, O., Costa, R. D. D., & Maciel, W. J. 2015, In preparation
- Chen, Y. Q., Zhao, G., Carrell, K., & Zhao, J. K. 2011, *AJ*, 142, 184
- Cheng, J. Y., et al. 2012a, *ApJ*, 746, 149
- Cheng, J. Y., Rockosi, C. M., & Morrison, H. L. 2012b, Galactic Archaeology: Near field cosmology and the formation of the Milky Way, ASP-CS 458, ed. W. Aoki et al.
- Chiappini, C., Minchev, I., Anders, F., Brauer, D., Boeche, C., & Martig, M. 2015, in Proc. of the workshop Asteroseismology of stellar populations in the Milky Way, Astrophysics and Space Science Proceedings, Volume 39, eds. A. Miglio, L. Girardi, P. Eggenberger, J. Montalbán, Springer, 111
- Curir, A., Lattanzi, M. G., Spagna, A., Matteucci, F., Morante, G., Fiorentin, P. R., & Spitoni, E. 2012, *A&A*, 545, A133
- Gibson, B. K., Pilkington, K., Bailin, J., Brook C. B., & Stinson, G. S. 2013, Nuclei in the Cosmos XII, Proc. of Science, [http://pos.sissa.it/archive/conferences/146/190/NIC%20XII\\_190.pdf](http://pos.sissa.it/archive/conferences/146/190/NIC%20XII_190.pdf)
- Gutenkunst, S., Bernard-Salas, J., Pottasch, S. R., Sloan, G. C., & Houck, J. R. 2008, *ApJ*, 680, 1206
- Henry, R. B. C., Kwitter, K. B., Jaskot, A. E., Balick, B., Morrison, M. B., & Milingo, J. B. 2010, *ApJ*, 724, 748
- Maciel, W. J. & Costa, R. D. D. 2013, *RMxAA*, 49, 333
- Maciel, W. J. & Costa, R. D. D. 2014, Asymmetrical planetary nebulae VI, ed. C. Morisset, G. Delgado-Inglada, S. Torres-Peimbert <http://www.astroscu.unam.mx/apn6/PROCEEDINGS/>
- Maciel, W. J., Costa, R. D. D., & Idiart, T. E. P. 2010, *A&A*, 512, A19
- Maciel, W. J., Costa, R. D. D., & Rodrigues, T. S. 2013, ESO Workshop, The Deaths of Stars and the Lives of Galaxies [http://www.eso.org/sci/meetings/2013/DSLG/Presentations/S\\_I-Maciel.pdf](http://www.eso.org/sci/meetings/2013/DSLG/Presentations/S_I-Maciel.pdf)
- Maciel, W. J., Rodrigues, T. S., & Costa, R. D. D. 2011, *RMxAA*, 47, 401
- Minchev, I., Chiappini, C., & Martig, M. 2014, *A&A*, 572, A92
- Nordström, B., Mayor, M., Andersen, J. et al. 2004, *A&A*, 418, 989
- Peimbert, M. 1978, IAU Symp. 76, ed. Y. Terzian (Dordrecht: Reidel), 215
- Pilkington, K., Few, C. G., Gibson, B. K., Calura, F. et al. 2012, *A&A*, 540, A56
- Sancho Miranda, M., Pilkington, K., Gibson, B. K., et al. 2014, Nuclei in the Cosmos XIII, poster 22
- Schönrich, R. & Binney, J. 2009, *MNRAS*, 399, 1145
- Spitoni, E., & Matteucci, F. 2011, *A&A*, 531, A72
- Stanghellini, L. & Haywood, M. 2010, *ApJ*, 714, 1096
- Stanghellini, L., Shaw, R. A., & Villaver, E. 2008, *ApJ*, 689, 194

O. Cavichia: Instituto de Física e Química, Universidade Federal de Itajubá, Av. BPS 1303, Pinheirinho, CEP 37500-903, Itajubá, MG, Brazil (cavichia@unifei.edu.br).

W. J. Maciel, & R. D. D. Costa: Instituto de Astronomia, Geofísica e Ciências Atmosféricas, Universidade de São Paulo - Rua do Matão 1226, CEP 05508-090, São Paulo SP, Brazil (wjmaciel@iag.usp.br, roberto.costa@iag.usp.br).